HHS Public Access

Author manuscript

Eur J Neurosci. Author manuscript; available in PMC 2016 March 01.

Published in final edited form as:

Eur J Neurosci. 2015 March ; 41(6): 748–759. doi:10.1111/ejn.12822.

Identification of a direct GABAergic pallidocortical pathway in rodents

Michael C. Chen[1,*], **Loris Ferrari**[1], **Matthew D. Sacchet**[2,3], **Lara C. Foland-Ross**[2], **Mei-Hong Qiu**[1], **Ian H. Gotlib**[2,3], **Patrick M. Fuller**[1], **Elda Arrigoni**[1], and **Jun Lu**[1,*]

[1]Department of Neurology, Beth Israel Deaconess Medical Center and Harvard Medical School, 3 Blackfan Circle Boston, MA, 02115

[2]Department of Psychology, Stanford University

[3]Neurosciences Program, Stanford University 420 Serra Mall Stanford, CA, 94305

Abstract

The basal ganglia, interacting with the cortex, play a critical role in a range of behaviors. Output from the basal ganglia to the cortex is thought to relay through the thalamus, yet an intriguing alternative is that the basal ganglia may directly project to, and communicate with, the cortex. We explored an efferent projection from the globus pallidus externa (GPe), a key hub in the basal ganglia system, to the cortex of rats and mice. Anterograde and retrograde tracing revealed projections to the frontal premotor cortex, especially the deep projecting layers, originating from GPe neurons that receive axonal inputs from the dorsal striatum. *Cre*-dependent anterograde tracing in GPe Vgat-ires-cre mice confirmed that the pallidocortical projection is GABAergic, and *in vitro* optogenetic stimulation in the cortex of these projections produced a fast inhibitory postsynaptic current in targeted cells that was abolished by bicucculine. The pallidocortical projections targeted GABAergic interneurons and, to a lesser extent, pyramidal neurons. This GABAergic pallidocortical pathway directly links the basal ganglia and cortex and may play a key role in behavior and cognition in normal and disease states.

Introduction

The basal ganglia are a collection of heterogeneous forebrain structures that play a critical role in motor behavior, cognition, affect, and sleep-wake regulation. One model of basal ganglia function proposes direct and indirect pathways for processing cortical information within the basal ganglia for output back to the cortex (Albin *et al.*, 1989). In both pathways, basal ganglia output to cortex is via thalamic relays, either directly from the striatum to globus pallidus interna (GPi) and substantia nigra reticulata (SNr), or indirectly via the globus pallidus externa (GPe), the subthalamic nucleus (STN), and the GPi/SNr. This model of basal ganglia function provides an interpretative framework for understanding the

[*]Corresponding authors contact information: Michael C. Chen, Beth Israel Deaconess Medical Center, 3 Blackfan Circle, CLS 717, Boston, MA, 02115, mcchen@alumni.stanford.edu, Jun Lu, Beth Israel Deaconess Medical Center, 3 Blackfan Circle, CLS 709, Boston, MA, 02115, jlu@bidmc.harvard.edu.

The authors report no conflict of interest.

etiology and pathogenesis of such disorders as Parkinson's disease, but it is insufficient to explain many pathological features of these diseases (Obeso *et al.*, 2008).

Basal ganglia structures like the GPe have robust connections within the basal ganglia, receiving striatal and subthalamic inputs and projecting back to these structures and the SNr and GPi, connecting every input and output structure of the basal ganglia (Kita, 2007). Basal ganglia output to the cortex, however, are thought to be primarily mediated by basal ganglia-thalamus-cortex relays. Deep brain stimulation of the STN and GPe ameliorates symptoms Parkinson's disease (Vitek *et al.*, 2012), but stimulation of the thalamus, the putative output relay for the basal ganglia, improves tremor but not necessarily bradykinesia and rigidity (Fasano *et al.*, 2012). Studies of the role of the basal ganglia in sleep add further complexity to the interaction of basal ganglia structures and other brain regions. Lesions of the GPe, but not of the STN or SNr, produce profound increases in wakefulness and alter motor behavior in rats (Qiu *et al.*, 2010). In contrast, lesions of the thalamus have a minimal effect on overall sleep wake patterns (Fuller *et al.*, 2011). These findings suggest the intriguing hypothesis that the basal ganglia, specifically the GPe, project to and directly communicate with other structures in the brain to influence behavior. Retrograde tracing from the cortex has previously identified neurons located in the GPe projecting to the cortex, but no study has shown that these are GPe neurons of the basal ganglia, rather than part of basal forebrain cortically projecting neurons (Saper, 1984; Zaborszky *et al.*, 2013). GABAergic GPe neurons projecting directly to the cortex would denote a novel basal ganglia output pathway with a potentially unique role in regulating motor and premotor cortical activity.

To investigate the efferent projection targets of the GPe, we placed unilateral injections of an adeno-associated viral vector (AAV) expressing a channelrhodopsin(ChR2)-YFP fusion product into the GPe of rats. We combined retrograde and anterograde tracing to confirm the pallicortical pathway originates from GPe neurons, and we used AAV-ChR2 in Vgat-ires-cre mice to specify and differentiate novel GPe projections. Finally, we used *in vitro* optogenetic stimulation of these GABAergic GPe projections to explore their functional role in cortical control.

Materials and Methods

Tracer injections

Twelve adult male Sprague-Dawley rats, weighing 300–325g (Taconic, Hudson NY), and five adult female Vgat-ires-cre mice (Vong *et al.*, 2011) weighing 20–25g were used. Rats were individually housed, and mice were group housed, in temperature and humidity controlled rooms under 12:12hr light-dark cycles with ad libitum access to food and water. Animal care was in accordance with National Institutes of Health standards with measures to minimize pain and discomfort, and all procedures used were approved by the Beth Israel Deaconess medical Center Institutional Animal Care and Use Committee. Rats and mice were weighed, then anesthetized with an i.p. injection of ketamine (100mg/kg) xylazine (10mg/kg) mix and placed into a stereotaxic frame. The cranium was exposed for measurement of coordinates relative to bregma, and a burr hole was made for injections. A 1mm glass pipette with a 10–20μm tapered tip was inserted into the brain at the calculated coordinates. Injections were made using electronically controlled air puffs lasting 5–10ms at

1–2 Hz. Injection volume was determined by measuring the meniscus of the injection liquid within the pipette using calibrated reticules on a surgical microscope. After 5 minutes of waiting to prevent backflow, the pipette was raised. After all injections, the scalp wound was closed with surgical clips, and the rodents were given meloxicam (5mg/kg) subcutaneously once daily for two days.

We used at least five rodents in each tracing group to ensure the consistency of the neuroanatomic pathways described; none of the rodents had any previous procedures. In six rats, we placed unilateral injections (24nL) of EF1a- hChR2 (H134R)-eYFP-AAV10 into the globus pallidus externa (GPe) [AP = −1.0mm, ML = −3.2mm, DV = −5.2mm (Paxinos & Watson, 2004)]. In six rats, we placed unilateral injections of fluorogold (120nL) into Fr2 [AP = 3.2mm, ML = 2.0mm, DV = −1mm] as well as in two of these rats unilateral injections of biotinylated dextran amine (45nL) into the dorsal striatum (CPu) [AP = −1.7, ML = 2.8mm, DV = −4.2mm]. For mice, we placed unilateral injections (15nL) of EF1a-DIO-hChR2 (H134R)-eYFP-AAV10 into the GPe [AP = −0.35mm, ML = −1.8mm, DV = −3.3mm (Franklin & Paxinos, 2008)]. All AAV-ChR2(H134R)-YFP were generously provided by Dr. Karl Deisseroth and were packaged into AAV10. The vector stocks were titered by real-time PCR using an Eppendorf Realplex machine. The titer of the preparations ranged from approximately 1×10^{12} to 1×10^{13} vector genomes copies/ml.

Immunohistochemistry

At least two weeks after injection, animals were deeply anesthetized with 7% chloral hydrate and perfused with 10% buffered formalin (Fisher Scientific, Pittsburgh PA). Brains were transferred to a solution of 20% sucrose and PBS containing 0.02% sodium azide overnight then sliced into four series of 40um sections using a freezing microtome. To stain, we incubated tissue in primary polyclonal anti-GFP 1:20,000 (Invitrogen A-6455, Lot 622086) or anti-fluorogold 1:10,000 (Chemikon AB153) for 24 hours followed by a 1 hour incubation in biotinylated secondary antiserum in PBST (Vector Laboratories). After washing with PBS, tissue was incubated with an avidin-biotin-horseradish peroxidase conjugate (Vector laboratories) and stained brown with 0.05% 3,3-diaminobenzidine tetrahydrochloride (Sigma, St. Louis MO) and 0.02% H2O2, or black with the addition of 0.05% cobalt chloride and 0.01% nickel ammonium sulfate. Sections were then mounted onto slides, some sections stained with 0.1% Thionin (Sigma, St Louis MO), dehydrated, and coverslipped.

Grayscale figures are presented using the monochrome with a blue filter in Adobe Photoshop, which minimizes the blue channel dominated by the thionin Nissl staining while preserving the black or brown staining for better visualizing projections from the injection site. To quantify staining intensity, we inverted the grayscale figures, marked cortical subregion boundaries, and measured pixel intensity in ImageJ on a 200 pixel line drawn from the edge of the cortex to the white matter in each cortical subregion. Intensity was normalized to the average of all measured subregions and distance from edge of cortex was normalized to each measurement.

Whole cell *in vitro* experiments

Vgat-ires-cre, lox-GFP (n = 7) mice [8 weeks, 20–25g] were used for *in vitro* electrophysiological recordings. This number of mice was used to successfully record a sufficient number of Fr2 neurons to functionally characterize the pallidocortical pathway. These mice were injected bilateraly in the the GPe [AP = −0.35mm, ML = −1.8mm, DV = −3.3mm] with EF1a-DIO-hChR2 (H134R)-eYFP-AAV10 (15 nL). 4 weeks after these injections, mice were used for *in vitro* electrophysiological recordings. Mice were anesthetized (ketamine 150 mg/kg and xylazine 15 mg/kg, i.p.) and transcardially perfused with ice-cold ACSF (*N*-methyl-D-glucamine, NMDG-based solution) containing (in mM): 100 NMDG-Cl, 2.5 KCl, 1.24 NaH_2PO_4, 30 $NaHCO_3$, 20 HEPES, 25 glucose, 2 thiourea, 5 Na-ascorbate, 3 Na-pyruvate, 0.5 $CaCl_2$, 10 $MgSO_4$ (pH 7.3 with HCl when carbogenated with 95% O_2 and 5% CO_2). Their brains were quickly removed and cut in coronal frontal cortical slices (250 μm thick) using a vibrating microtome (VT1000, Leica, Bannockburn, IL, USA). Slices containing the Fr2 were transferred in normal ACSF (Na-based solution) containing (in mM): 120 NaCl, 2.5 KCl, 10 glucose, 26 $NaHCO_3$, 1.24 NaH_2PO_4, $MgCl_2$ 1.3, 4 $CaCl_2$, 2 thiourea, 1 Na-ascorbate, 3 Na-pyruvate, 1 Kynurenic acid (pH 7.4 when carbogenated with 95% O_2 and 5% CO_2, 310–320 mOsm).

Recordings were made from 17 GFP(+) and 19 pyramidal cells in the deep layers (V/VI) of the Fr2 premotor cortex from 7 mice. On average, 5 neurons per mouse were recorded (ranging from 4 to 7 per animal). Recordings were guided using a combination of fluorescence and infrared differential interference contrast (IR-DIC) video microscopy using a fixed stage upright microscope (BX51WI, Olympus America Inc.) equipped with a Nomarski water immersion lens (40×/ 0.8 W) and IR-sensitive CCD camera (ORCA-ER, Hamamatsu, Bridgewater, NJ, USA) and images were displayed on a computer screen in real time using AxioVision software (Carl Zeiss MicroImaging). Recordings were conducted in whole-cell configuration, at room temperature using a Multiclamp 700B amplifier (Molecular Devices, Foster City, CA, USA), a Digidata 1322A interface and Clampex 9.0 software (Molecular Devices). GP axons and synaptic terminals expressing ChR2 were activated by a full-field 5 ms flashes of light (~ 10 mW/mm^2 1mm beam width) from a 5 W luxeon blue light-emitted diode (470 nm wavelength; #M470L2-C4; Thorlabs, Newton, NJ, USA) coupled to the epifluorescence pathway of the Zeiss microscope. The area stimulated included the recorded cell, which is in the center of a 500 μm radius concentric field. Photo-evoked IPSCs were recorded at Vh = −40 mV using a K gluconate-based pipette solution containing (in mM): 120 K-gluconate, 10 KCl, 10 HEPES, 3 $MgCl_2$, 5 K-ATP, 0.3 Na-GTP and 0.5% biocytin (pH adjusted to 7.2 with KOH, 280 mOsm). Liquid junction potential was calculated to be +13.2 mV and all recordings were not corrected for it.

Electrophysiological data were analyzed using Clampfit 9.0 (Molecular Devices) and IGOR Pro 6 (WaveMetrics, Lake Oswego, OR, USA). Synaptic events were detected off-line using Mini Analysis 6 (Synaptosoft, Leonia, NJ, USA). Action potential (AP) duration was calculated as the width at the voltage halfway between the AP threshold and the AP peak and AP threshold was calculated as the voltage at which the slope of the AP reached ≥ 20 V s^{-1}. The latency of the photo-evoked IPSCs was determined by the time difference between the starting of the light pulse and the 5% rise point of the first IPSC. Results are expressed as

mean ± S.E.M. and *n* refers to the number of cells. Immediately following the *in vitro* recordings, recorded slices and slices containing the injection site were fixed in 10% buffered formalin (overnight), then cryoprotected in 40% sucrose and re-sectioned into 60 μm sections on a freezing microtome. We examined the sections under fluorescence to verify the location the extent of ChR2-YFP expressing neurons in the injection sites, as the GPe injection site clearly shows dense fibers and terminals in addition to the native GFP fluorescence. We then incubated the sections overnight in an avidin-biotin-horseradish peroxidase conjugate (ABC, Vector laboratories) and stained back with 0.05% 3,3-diaminobenzidine tetrahydrochloride (DAB; Sigma, St. Louis MO), 0.02% H_2O_2, 0.05% cobalt chloride and 0.01% nickel ammonium sulfate. Sections were then mounted onto slides, dehydrated, and coverslipped.

Statistical Analysis

For analysis of the response rate of pyramidal ($n = 19$) and non-pyramidal neurons ($n = 17$), we compared the proportion of responding and non-responding neurons of each type with Fisher's exact test (GraphPad).

Results

Rat GPe projections

In all six rats tested, tracer injections filled cell bodies and local fibers within the anterior GPe without filling cells in the BF (Figure 1, Figure 2A–C). Starting from the rostrocaudal level of the GPe, we observed in all rats innervation of the secondary motor cortex / frontal cortex (Fr2), an anatomical region also known as the agranular medial cortex, medial precentral area, or secondary motor area (Uylings *et al.*, 2003). The projections were ipsilateral, passing through the striatum and terminating in Fr2 (Figure 2A). Fr2 projections were sparse at the level of the injection, increasing in density in rostral sections (Figure 2B–C), and reaching their greatest density at the rostral extent of the striatum (Figure 2D). GPe projections reached the most rostral parts of the forebrain (Figure 2E–F), spreading laterally in frontal regions while remaining sparse in the medial wall and orbital regions (Figure 2F). Projections to Fr2 appeared topographic, with more lateral injections within the GPe producing more lateral projections to both the striatum and Fr2 region. However, projections always targeted Fr2 while avoiding the anterior cingulate cortex. No cell bodies were stained in the cortex.

To quantify the cortical projections, we inverted the grayscale images and measured the staining intensity of projections within cortical subregions in three representative coronal sections (Figure 3). At a level anterior to the striatum (Figure 3A–B), projections—including fibers and terminals—are heaviest in Fr2, followed by lighter staining in the adjacent M1 and cingulate cortex, some staining in the anterior insula, and almost no projections in the prelimbic or sensory cortices. At the anterior tip of the striatum (Figure 3C–D), the heaviest staining is seen in Fr2, with staining also seen in adjacent M1 and anterior insula. Little or no staining was observed in prelimbic, cingulate, or sensory cortices. In the rostral striatum (Figure 3E–F), staining is heaviest in Fr2, with some projections in M1 and anterior insula,

and little staining elsewhere. In general, heavier projections are seen in more anterior sections, and no projections were observed caudal to injection site.

Projections in Fr2, were densest in the deep projection layer V of the cortex (Figure 3A,C,E; Figure 4D), although terminal boutons were observed from the level of the injection site to the rostral extent of the cortex (see insets, Figure 1A–F) in both superficial (Figure 4B) and deep layers (Figure 4C). Pallidocortical projections were sparse or absent in primary motor cortex and other cortical regions. Dense GPe projections were observed in STN, entopedunclear nucleus (EPN/GPi), and substantia nigra pars reticulata (SNr) and pars compacta (SNc), (Figure 4D–F), as well as in the striatum (Figure 1A–C), consistent with previous reports of GPe projections (Kita, 2007). Bilateral projections, with ipsilateral predominance, were also observed in the reticular, mediodorsal, parafascicular, and centrolateral nuclei of the thalamus (Figure 4G).

Striatal projections to pallidocortical neurons

Neurons in the basal forebrain (BF) located ventral to the GPe have glutamatergic, GABAergic, and cholinergic projections throughout the cortex (Saper, 1984; Gritti *et al.*, 1997; Henny & Jones, 2008), but these neurons do not receive striatal input. To differentiate GPe projections to the cortex from BF projections in the cortex, we injected a retrograde fluorogold tracer (stained brown) into Fr2 in rats (Figure 5A) in 6 rats, along with in 2 rats an anterograde biotinylated dextran amine tracer (stained black) into the rostral dorsal striatum (Figure 5B), which projects to the GPe but not the BF. Consistent with ChR2 tracing of the pallidocortical pathway, we observed retrogradely labeled neurons throughout the GPe (see representative tracing in Figure 5C) in all 6 rats, as well as neurons in the BF. In rats with anterograde tracing, neurons in the GPe also received projections from striatum neurons (Figure 5D–H). Extended focus microscopy revealed striatal terminal boutons appearing on cell bodies and dendrites of the GPe neurons that were retrogradely labeled from Fr2. Conversely, BF neurons ventral to the GPe did not receive any projections from the striatum (Figure 5I).

Mouse GABA GPe projections

GPe neurons are mostly GABAergic, but non-GABAergic neurons, especially cholinergic GPe neurons, are thought to project to the cortex (Walker *et al.*, 1989; Moriizumi & Hattori, 1992). To differentiate GABAergic GPe projections observed in the rats from cholinergic projections of the GPe (Saper, 1984), we injected cre-dependent EF1a-DIO-hChR2 (H134R)-eYFP-AAV10 into the GPe Vgat-ires-cre mice (Figure 6A–B).

Consistent with rat pallidocortical projections, we observed in all injected mice GABAergic GPe fiber projections to Fr2, beginning near the rostral-caudal level of the GPe (see representative tracing in Figure 7A) and becoming heaviest at the level of the most rostral aspect of the striatum (Figure 7B–D). Projections were also observed at the most rostral aspect of the forebrain, becoming sparser along the ventral medial wall (Figure 7E–F). Notably, GABAergic BF neurons at this level project to the infralimbic (Henny & Jones, 2008) and somatosensory cortices (Gritti *et al.*, 1997); we did not observe similar innervation of the infralimbic or somatosensory cortices by GABAergic GPe neurons.

To quantify these GABAergic projections, we measured staining intensity of projections—fibers and terminals—within cortical subregions in three representative coronal sections (Figure 8). At a level anterior to the striatum (Figure 8A–B), projections are heaviest in Fr2, followed by lighter staining in the cingulate cortex and M1, with few projections in the anterior insula, prelimbic, or sensory cortices. At the anterior tip of the striatum (Figure 8C–D), the heaviest staining is seen in Fr2, with staining also seen in adjacent M1 and cingulate cortex, with lighter or no staining in prelimbic, cingulate, or sensory cortices. In the rostral striatum (Figure 8E–F), staining is heaviest in Fr2, with some projections in M1, cingulate cortex, and anterior insula, and little staining elsewhere. In Fr2 and adjacent subregions, the most intense staining was observed in deeper, projection layers of the cortex, and as in rats, heavier projections are seen in more anterior sections. No cortical projections were seen caudal to the injection site. As in rats, GPe fibers and boutons in Fr2 were heaviest in layers V and VI, although fibers and terminals were found throughout all layers of cortex (Figure 9A–C).As in rats, GPe injections of DIO-hChR2-eEYP revealed fibers and terminals in the STN, EPN/GPi, SNr, and striatum, as well as mediodorsal, centrolateral, parafascicular, and reticular thalamus (Figure 9D–G).

In vitro optogenetic characterization of pallidocortical projections

To confirm the GABAergic pallidocortical projections, and to characterize the functional targets of these projections, we injected EF1a-DIO-hChR2 (H134R)-eYFP-AAV10 into the GPe of five *Vgat*-ires-cre-GFP mice. We recorded from GABAergic/GFP-expressing neurons and pyramidal neurons of layers V/VI of Fr2 (Figure 10A), as these deep layers receive the strongest pallidocortical projections (Figures 3, 8). Under IR visualization GABAergic/GFP-expressing neurons had a round soma quite distinctive from the neighboring pyramidal cells (Figure 10B), were silent with at resting membrane potential (−53.93 ± 2.6 mV) and had an input resistance of 208.18 ± 28.65 MΩ (n = 10). These neurons responded to depolarizing current steps with a fast and high frequency firing (Figure 10C). They also displayed a narrow action potential (AP width: 0.61 ± 0.04 ms) followed by a large afterhyperpolarization (AHP; −19.53 ± 2.13 mV; n = 10). They responded to hyperpolarizing pulses with a small voltage-dependent rectification and a small depolarizing sag, suggesting the presence of an inwardly-rectifying I_K and an I_h.

Photostimulation of axons and terminals that originated from GPe^{Vgat} neurons evoked release of GABA that inhibits the firing of GFP(+) Fr2 neurons. This effect was blocked by bicuculline (10 μM, Figure 10D) indicating that these responses were mediated by activation of $GABA_A$ postsynaptic receptors. In voltage-clamp recordings photostimulation of GPe^{Vgat} axons/terminals evoked fast inhibitory postsynaptic currents (IPSCs) in GFP(+) Fr2 neurons (n = 10 of 17 neurons, Figure 10E–I) that were completely abolished by bicuculline. The peak amplitude of the photoevoked IPSCs was 34.57 ± 11.3 pA and IPSC rise and decay could be fit with single exponentials (rise time constant: 1.9 ± 0.3 ms and decay time constant: 13.57 ± 1.98 ms) (Figure 10H). Paired pulse tests (80 ms inter-pulse intervals) showed robust paired pulse depression (76%; n = 2) suggesting high release probability of $GPe^{Vgat}\rightarrow Fr2^{GFP(+)}$ input (Figure 10I). In addition, onset delay of the photo-evoked IPSCs was short (4.38 ± 0.28 ms; Figure 10G) supporting a direct synaptic connectivity from GPe to Fr2 GABAergic interneurons.

We also recorded from 19 pyramidal cells in the same layers of the Fr2 cortex. These neurons were identified based on their shape and their firing properties (Figure 10J–K). Photo-stimulation of GPe^{Vgat} axons and terminals evoked IPSCs in 3 out of 19 pyramidal neurons (Figure 10L). The peak amplitude of the photo-evoked IPSCs in these 3 pyramidal cells was 15.4 ± 6.2 pA, and importantly the onset delay of the photo-evoked IPSCs was short (5.19 ± 0.62 ms), supporting a direct synaptic connectivity from GPe to Fr2 pyramidal cells.

Overall, optogenetic activation of GPe^{Vgat} projections evoked inhibitory synaptic responses in a greater proportion of Fr2 GABAergic neurons (58.8%) than Fr2 pyramidal neurons (15.8%, *Fisher's exact test P = 0.01*). These results indicate that functional GPe^{Vgat} projections target Fr2 neurons, primarily GABAergic interneurons and some pyramidal cells.

Discussion

Using a ChR2-based tracer in rats, we found ipsilateral projections from the GPe to all cortical layers, especially to the pyramidal cell-containing layer V, of Fr2, also known as the secondary motor cortex or M2. We confirmed that these are GPe neurons by retrogradely labeling from the Fr2 in combination with anterograde labeling from the CPu, revealing cortically-projecting GPe neurons innervated by CPu. We then showed using Vgat-ires-cre mice that these GPe projections to the cortex are GABAergic. Finally, we confirmed using *in vitro* optogenetic stimulation that these GABAergic pallidocortical projections can target neurons in the cortex and produce a rapid, inhibitory synaptic response that inhibits action potential firing. Taken together, these findings suggest that the GPe, and by extension the basal ganglia, projects directly to the cortex. While previous studies have retrogradely labeled neurons in the GPe from the cortex, (Van Der Kooy & Kolb, 1985), it was unclear whether these projections originated from GPe neurons rather than BF neurons, whether these projections targeted a specific cortical regions, and whether stimulation of this projection directly affected cortical neurons. The present study is the first to show that the cortically-projecting GPe neurons receive striatal projections and are thus part of a basal ganglia system that projects directly to the prefrontal cortex, especially deep layers of Fr2. Furthermore, the present study is the first to characterize a functional, inhibitory role of GABAergic pallidocortical projections on cortical neurons. This pallidocortical projection is a unique pathway for basal ganglia-cortical interaction.

Pallidocortical projections allow GABAergic neurons of the GPe, which receive projections from all basal ganglia input and output nuclei, to directly influence cortical activity. Quantification of staining intensity confirmed that the heaviest projection density is in Fr2, with some additional projections in adjacent cingulate and motor cortices--two regions immediately adjoining the Fr2--as well as the anterior insula. The projection field is wider in the most rostral parts of the prefrontal cortex, where the precise delineation of Fr2 and other regions is unclear (Uylings *et al.*, 2003). In contrast, the GPe does not send heavy projections to orbital, infralimbic, prelimbic, or sensory regions, nor do projections target motor or premotor regions caudal to the injection site, although the caudal GPe may have additional cortical targets. Just as CPu anterograde tracing targeted a specific region of the

GPe, cortically projecting GPe neurons target Fr2 in the rostral cortex and striatum in a topographic manner. GPe projections to the cortex, basal ganglia, and thalamus (Gandia *et al.*, 1993) enable the GPe to influence multiple circuits throughout the brain.

Fr2 has been compared to the frontal cortex of primates, although there is debate concerning the precise mapping of homologous primate and rodent frontal regions(Preuss, 1995; Uylings *et al.*, 2003; Wise, 2008). The Fr2 region specifically has been implicated in a range of functions, particularly those shaping the selection and initiation of action (Grillner *et al.*, 2005; Sul *et al.*, 2011). Much as the GPe is a hub of basal ganglia activity, Fr2 receives input from somatosensory and other cortical regions (Condé *et al.*, 1995) while projecting to motor cortex. Through the pallidocortical pathway, the GPe is likely able to play a direct role in behavior, such as modulation of Fr2 activity to adapt to reward contingencies (Kargo *et al.*, 2007). Because GPe projections to other cortical regions are so limited, we hypothesize that the pallidocortical pathway is a specialized circuit for regulation of premotor and motor activity. In contrast, other cortically-projecting systems like the basal forebrain project widely throughout the cortex and modulate global patterns of cortical activity. The pallidcortical pathway bridges two regions that in turn integrate inputs and outputs from the basal ganglia and cortex, respectively. This direct shortcut from basal ganglia to cortex may play a specialized role alongside basal ganglia-thalamic-cortical loops.

Our *in vitro* experiments indicate that the pallidocortical pathway preferentially targets GABAergic neurons in Fr2, presumably interneurons. These putative interneurons had firing properties resembling fast spiking GABAergic / parvalbumin (+) cortical interneurons (Cauli *et al.*, 1997) which account for almost 50% of neocortical GABAergic cells in layers V and VI (Rudy *et al.*, 2011). We also found that GPe project to pyramidal cells, although the proportion of responding pyramidal neurons is less than GABAergic neurons. And although we focused on deep layers projections, pallidocortical projections to superficial layers may also contribute to GPe modulation of cortical activity. GPe neurons may help set cortical firing rates via direct input to cortical interneurons as well as indirect input to pyramidal cells or via the indirect basal ganglia pathway. Future work must delineate the molecular and physiological properties of the origins and targets of pallidocortical neuron projections, both within the known organization of GPe neurons (Nóbrega-Pereira *et al.*, 2010; Mallet *et al.*, 2012; Mastro *et al.*, 2014) and cortical architecture.

Cholinergic and GABAergic BF neurons project widely throughout the cortex, sharing many developmental, anatomic, and functional characteristics with the GPe. Retrograde tracing studies from Fr2 show projections originating not only from BF populations but also from within the GPe itself (Zaborszky *et al.*, 2013). Unlike BF neurons, which project diffusely across the cortex, output from the GABAergic pallidocortical pathway is concentrated on Fr2 and avoids other BF targets, including the amygdala and lateral hypothalamus. While our retrograde tracing from Fr2 reveals BF innervation of the cortex, these neurons—located ventral to the GPe—did not receive projections from the CPu. BF and GPe both contain GABA neurons that project to the cortex, and appear to be a continuous population based on retrograde tracing alone, especially at caudal levels, but only GPe neurons receive striatal input as part of the basal ganglia system. Delineating the similarities and differences in GPe

and BF physiology and anatomy will be critical to understanding how the basal ganglia and BF interact with the cortex. For example, while our *in vitro* experiments clearly indicate that the pallidocortical pathway has a GABAergic, inhibitory phenotype, the cholinergic neurons within the GPe may also contribute a cortical projection, although these neurons are sparse within the GPe at the rostral levels we examined (Walker *et al.*, 1989; Moriizumi & Hattori, 1992). It is unclear if these cholinergic neurons within the GPe or in the borders of the GPe receive CPu inputs.

In summary, we describe a GABAergic pallidocortical output pathway that directly links the basal ganglia and cortex. The rapid and inhibitory response produced by *in vitro* stimulation pallidocortical terminals supports a role for the GPe in shaping Fr2 firing patterns. Direct inhibitory GABAergic projections from the GPe to the projecting layers of Fr2 cortex may disinhibit premotor regions to influence motor planning and execution (Kargo *et al.*, 2007) or provide a direct route of propagating deleterious basal ganglia oscillations to the cortex, such as the abnormal oscillations in GPe-STN circuits present in Parkinson's disease (Mallet *et al.*, 2008; Obeso *et al.*, 2008). The identification of this pallidocortical circuit may provide a structural basis for understanding the pathologic motor features of basal ganglia disorders and suggests an important role for GPe-cortical dialogue in motor control.

Acknowledgment

The authors thank Quan Ha and Xi Chen for technical expertise. This work was supported by the Hilda and Preston Davis Foundation (M.C.C.) and National Institutes of Health (NS061863, NS082854 and HL095491 to E.A.; NS073613 to P.M.F.; NS062727 and NS061841 to J.L.).

References

Albin RL, Young AB, Penney JB. The functional anatomy of basal ganglia disorders. Trends Neurosci. 1989; 12:366–375. [PubMed: 2479133]

Cauli B, Audinat E, Lambolez B, Angulo MC, Ropert N, Tsuzuki K, Hestrin S, Rossier J. Molecular and physiological diversity of cortical nonpyramidal cells. J. Neurosci. 1997; 17:3894–3906. [PubMed: 9133407]

Condé F, Maire-Lepoivre E, Audinat E, Crépel F. Afferent connections of the medial frontal cortex of the rat. II. Cortical and subcortical afferents. J. Comp. Neurol. 1995; 352:567–593. [PubMed: 7722001]

Fasano A, Daniele A, Albanese A. Treatment of motor and non-motor features of Parkinson's disease with deep brain stimulation. The Lancet Neurology. 2012; 11:429–442. [PubMed: 22516078]

Franklin, KBJ.; Paxinos, G. The Mouse Brain: In Stereotaxic Coordinates. San Diego: Academic Press; 2008. [etc.].

Fuller PM, Fuller P, Sherman D, Pedersen NP, Saper CB, Lu J. Reassessment of the structural basis of the ascending arousal system. J. Comp. Neurol. 2011; 519:933–956. [PubMed: 21280045]

Gandia JA, De Las Heras S, García M, Giménez-Amaya JM. Afferent projections to the reticular thalamic nucleus from the globus pallidus and the substantia nigra in the rat. Brain Res. Bull. 1993; 32:351–358. [PubMed: 7693305]

Grillner S, Hellgren J, Ménard A, Saitoh K, Wikström MA. Mechanisms for selection of basic motor programs – roles for the striatum and pallidum. Trends in Neurosciences. 2005; 28:364–370. [PubMed: 15935487]

Gritti I, Mainville L, Mancia M, Jones BE. GABAergic and other noncholinergic basal forebrain neurons, together with cholinergic neurons, project to the mesocortex and isocortex in the rat. The Journal of Comparative Neurology. 1997; 383:163–177. [PubMed: 9182846]

Henny P, Jones BE. Projections from basal forebrain to prefrontal cortex comprise cholinergic, GABAergic and glutamatergic inputs to pyramidal cells or interneurons. Eur. J. Neurosci. 2008; 27:654–670. [PubMed: 18279318]

Kargo WJ, Szatmary B, Nitz DA. Adaptation of Prefrontal Cortical Firing Patterns and Their Fidelity to Changes in Action–Reward Contingencies. J. Neurosci. 2007; 27:3548–3559. [PubMed: 17392471]

Kita H. Globus pallidus external segment. Prog. Brain Res. 2007; 160:111–133. [PubMed: 17499111]

Mallet N, Micklem BR, Henny P, Brown MT, Williams C, Bolam JP, Nakamura KC, Magill PJ. Dichotomous Organization of the External Globus Pallidus. Neuron. 2012; 74:1075–1086. [PubMed: 22726837]

Mallet N, Pogosyan A, Márton LF, Bolam JP, Brown P, Magill PJ. Parkinsonian Beta Oscillations in the External Globus Pallidus and Their Relationship with Subthalamic Nucleus Activity. J. Neurosci. 2008; 28:14245–14258. [PubMed: 19109506]

Mastro KJ, Bouchard RS, Holt HAK, Gittis AH. Transgenic Mouse Lines Subdivide External Segment of the Globus Pallidus (GPe) Neurons and Reveal Distinct GPe Output Pathways. J. Neurosci. 2014; 34:2087–2099. [PubMed: 24501350]

Moriizumi T, Hattori T. Separate neuronal populations of the rat globus pallidus projecting to the subthalamic nucleus, auditory cortex and pedunculopontine tegmental area. Neuroscience. 1992; 46:701–710. [PubMed: 1372116]

Nóbrega-Pereira S, Gelman D, Bartolini G, Pla R, Pierani A, Marín O. Origin and Molecular Specification of Globus Pallidus Neurons. J. Neurosci. 2010; 30:2824–2834. [PubMed: 20181580]

Obeso JA, Marin C, Rodriguez-Oroz C, Blesa J, Benitez-Temiño B, Mena-Segovia J, Rodríguez M, Olanow CW. The basal ganglia in Parkinson's disease: current concepts and unexplained observations. Ann. Neurol. 2008; 64(Suppl 2):S30–S46. [PubMed: 19127584]

Paxinos, G.; Watson, C. The Rat Brain in Stereotaxic Coordinates - The New Coronal Set. Academic Press; 2004.

Preuss TM. Do Rats Have Prefrontal Cortex? The Rose-Woolsey-Akert Program Reconsidered. Journal of Cognitive Neuroscience. 1995; 7:1–24. [PubMed: 23961750]

Qiu M-H, Vetrivelan R, Fuller PM, Lu J. Basal ganglia control of sleep-wake behavior and cortical activation. Eur. J. Neurosci. 2010; 31:499–507. [PubMed: 20105243]

Rudy B, Fishell G, Lee S, Hjerling-Leffler J. Three groups of interneurons account for nearly 100% of neocortical GABAergic neurons. Dev Neurobiol. 2011; 71:45–61. [PubMed: 21154909]

Saper CB. Organization of cerebral cortical afferent systems in the rat. II. Magnocellular basal nucleus. The Journal of Comparative Neurology. 1984; 222:313–342. [PubMed: 6699210]

Sul JH, Jo S, Lee D, Jung MW. Role of rodent secondary motor cortex in value-based action selection. Nat Neurosci. 2011; 14:1202–1208. [PubMed: 21841777]

Uylings HBM, Groenewegen HJ, Kolb B. Do rats have a prefrontal cortex? Behavioural Brain Research. 2003; 146:3–17. [PubMed: 14643455]

Van Der Kooy D, Kolb B. Non-cholinergic globus pallidus cells that project to the cortex but not to the subthalamic nucleus in rat. Neuroscience Letters. 1985; 57:113–118. [PubMed: 4034088]

Vitek JL, Zhang J, Hashimoto T, Russo GS, Baker KB. External pallidal stimulation improves parkinsonian motor signs and modulates neuronal activity throughout the basal ganglia thalamic network. Exp. Neurol. 2012; 233:581–586. [PubMed: 22001773]

Vong L, Ye C, Yang Z, Choi B, Chua S Jr, Lowell BB. Leptin Action on GABAergic Neurons Prevents Obesity and Reduces Inhibitory Tone to POMC Neurons. Neuron. 2011; 71:142–154. [PubMed: 21745644]

Walker RH, Arbuthnott GW, Wright AK. Electrophysiological and anatomical observations concerning the pallidostriatal pathway in the rat. Exp Brain Res. 1989; 74:303–310. [PubMed: 2494050]

Wise SP. Forward frontal fields: phylogeny and fundamental function. Trends Neurosci. 2008; 31:599–608. [PubMed: 18835649]

Zaborszky L, Csordas A, Mosca K, Kim J, Gielow MR, Vadasz C, Nadasdy Z. Neurons in the Basal Forebrain Project to the Cortex in a Complex Topographic Organization that Reflects

Corticocortical Connectivity Patterns: An Experimental Study Based on Retrograde Tracing and 3D Reconstruction. Cereb. Cortex. 2013 bht210.

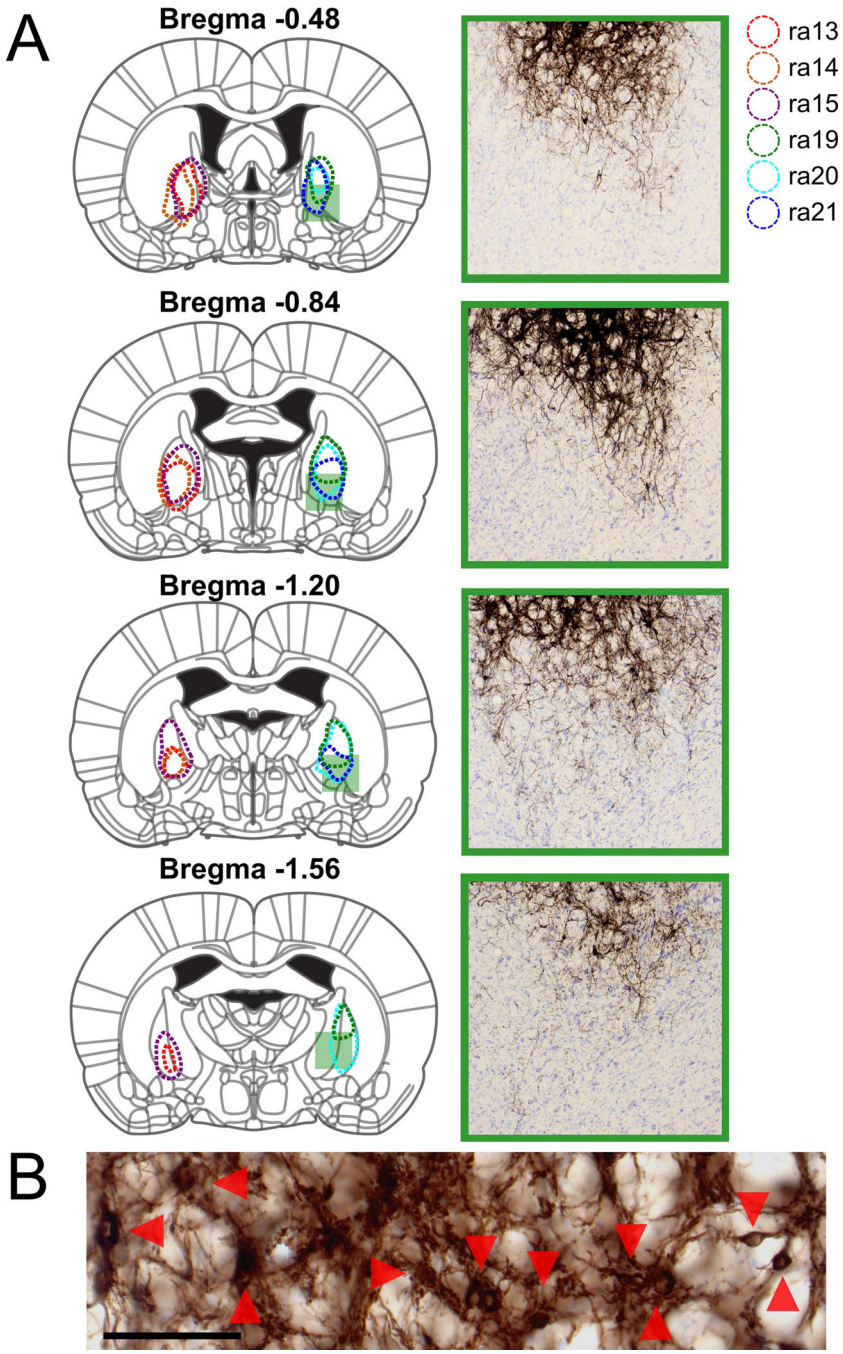

Figure 1. Injection sites of ChR2 into the rat GPe overlayed onto a standard rat atlas

(A) All injections were unilateral, and injection outlines are split between sides for visibility. Boxes, corresponding to case ra19 used in Figure 1, show a magnified image of the green square zones on the injection diagram. Magnified images show injections in the GPe and extensive fibers, with no filled cell bodies in the basal forebrain (BF). (B) Filled cell bodies in the GPe injection site. Scale bar: 100μm.

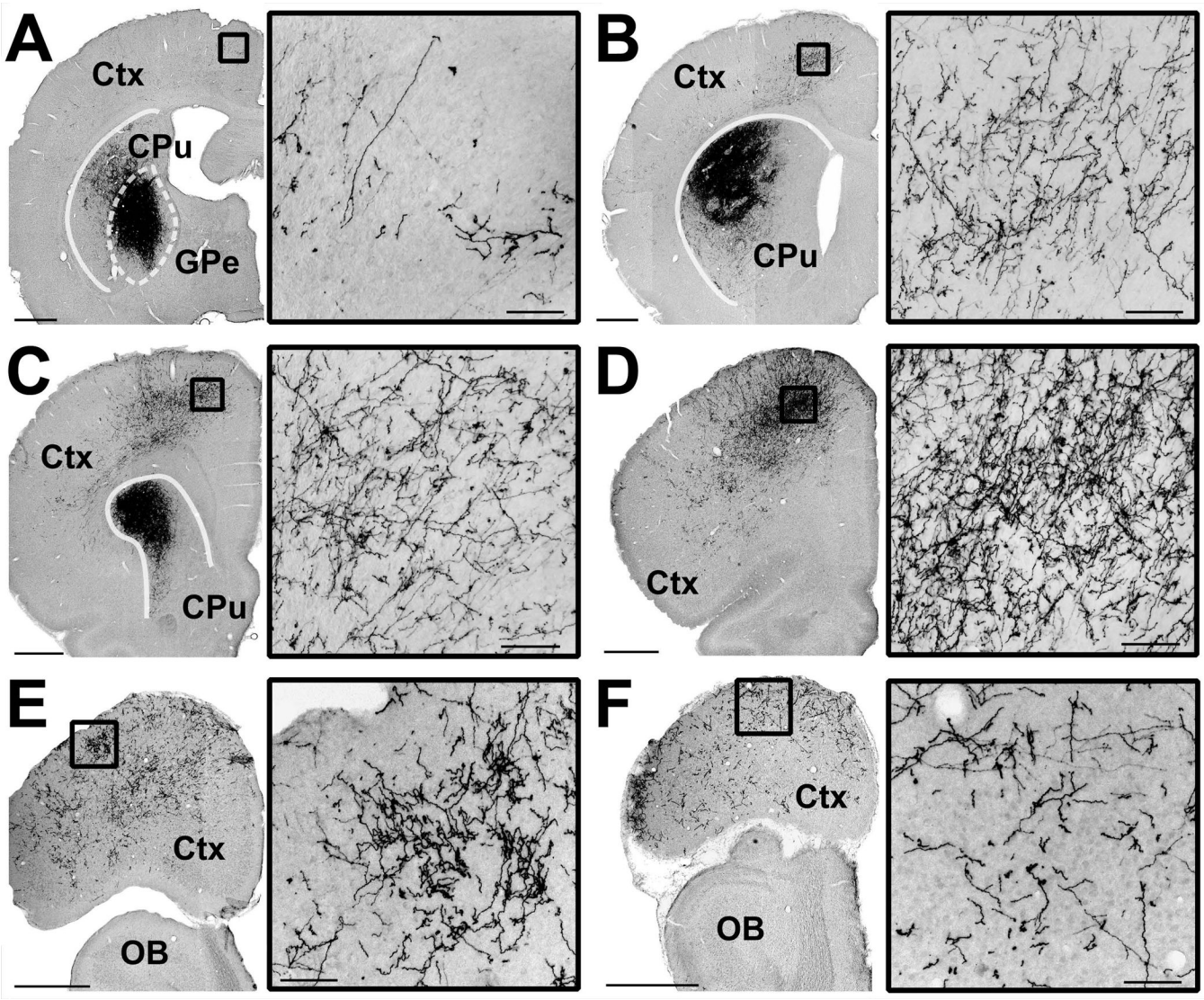

Figure 2. Tracer injection into the GPe, stained black against GFP, label projections to Fr2 cortex at levels rostral to the injection site

(A) At the level of the injection site, heavy staining is observed in the dorsal striatum, while sparse projections and terminals can be seen in the caudal extent of Fr2 (inset). (B) At the rostrocaudal level of striatum, GPe projections into the striatum and Fr2 (inset). (C) At the level of the rostral striatum, heavy GPe projections to both striatum and Fr2 are observed, with dense fibers and terminals throughout layers V and VI. GPe projections reached their heaviest level at the rostral extent of the striatum (D), with dense fibers and terminals through all layers (inset), while expanding laterally through the cortex (E) and reaching the most rostral extent of the cortex (F). Abbreviations: globus pallidus externa (GPe), striatum (CPu), cortex (Ctx), olfactory bulb (OB). Scale bars: A–F, 1mm; insets 100μm.

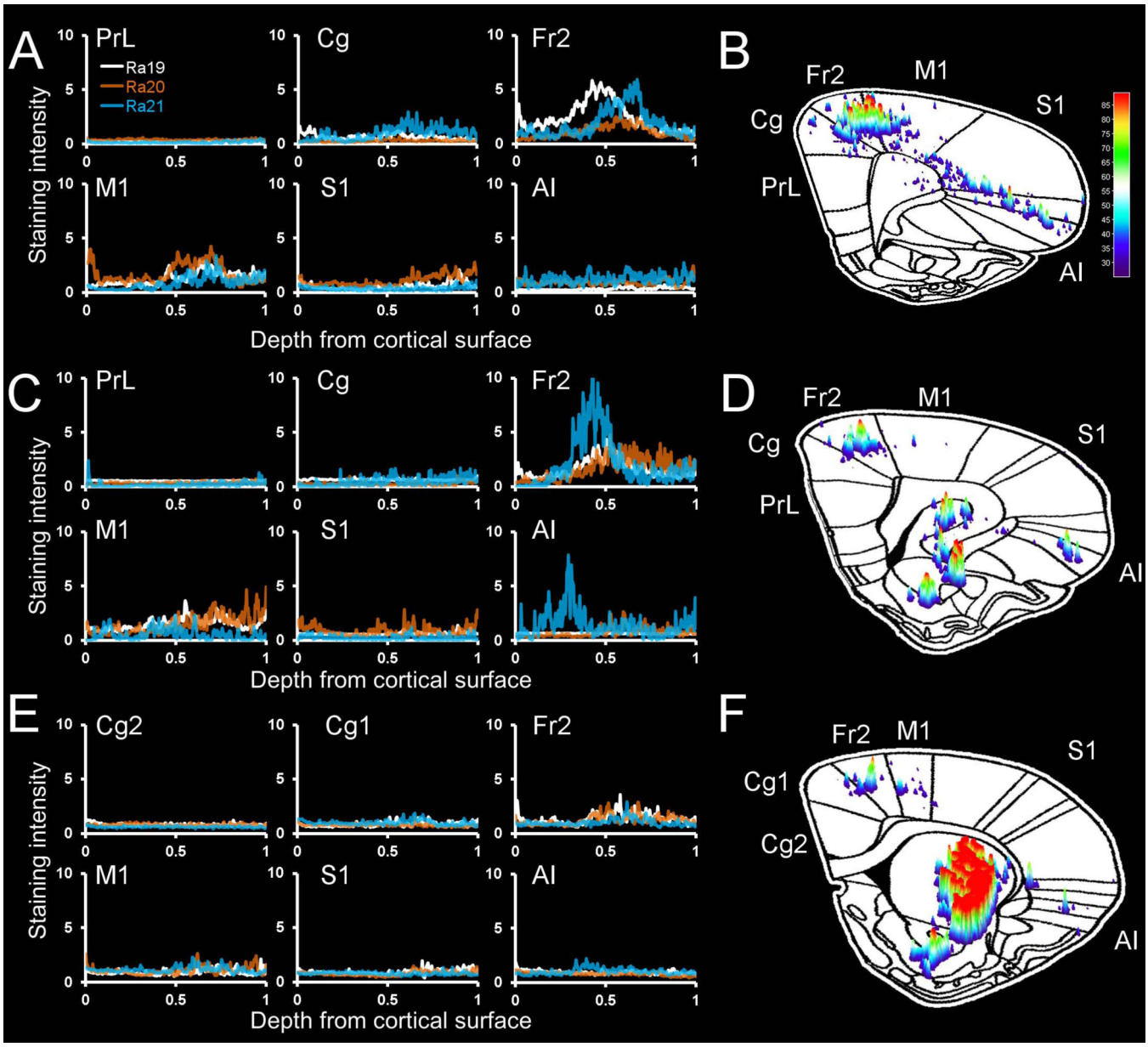

Figure 3. Quantitative mapping of GPe projections to cortical subregions in rats

Projection mapping in three representative rat cases, plotting normalized staining intensity against relative distance from the cortical surface to the white matter (A,C,E). Projection intensity from case Ra21 overlaid on a standardized mouse atlas (B,D,F) demonstrates the typical pattern of the GABAergic pallidocortical projection, with heavy projections to Fr2 and adjacent areas. Staining intensity of six major cortical areas are presented at the level anterior to the striatum (A–B), the anterior striatum (C–D), and striatum (E–F). Abbreviations: prelimbic cortex (PrL), cingulate cortex (Cg), frontal area 2 (Fr2), primary motor cortex (M1), primary somatosensory cortex (S1), anterior insula (AI). Colored bars in (B,D,F) reflect pixel intensity.

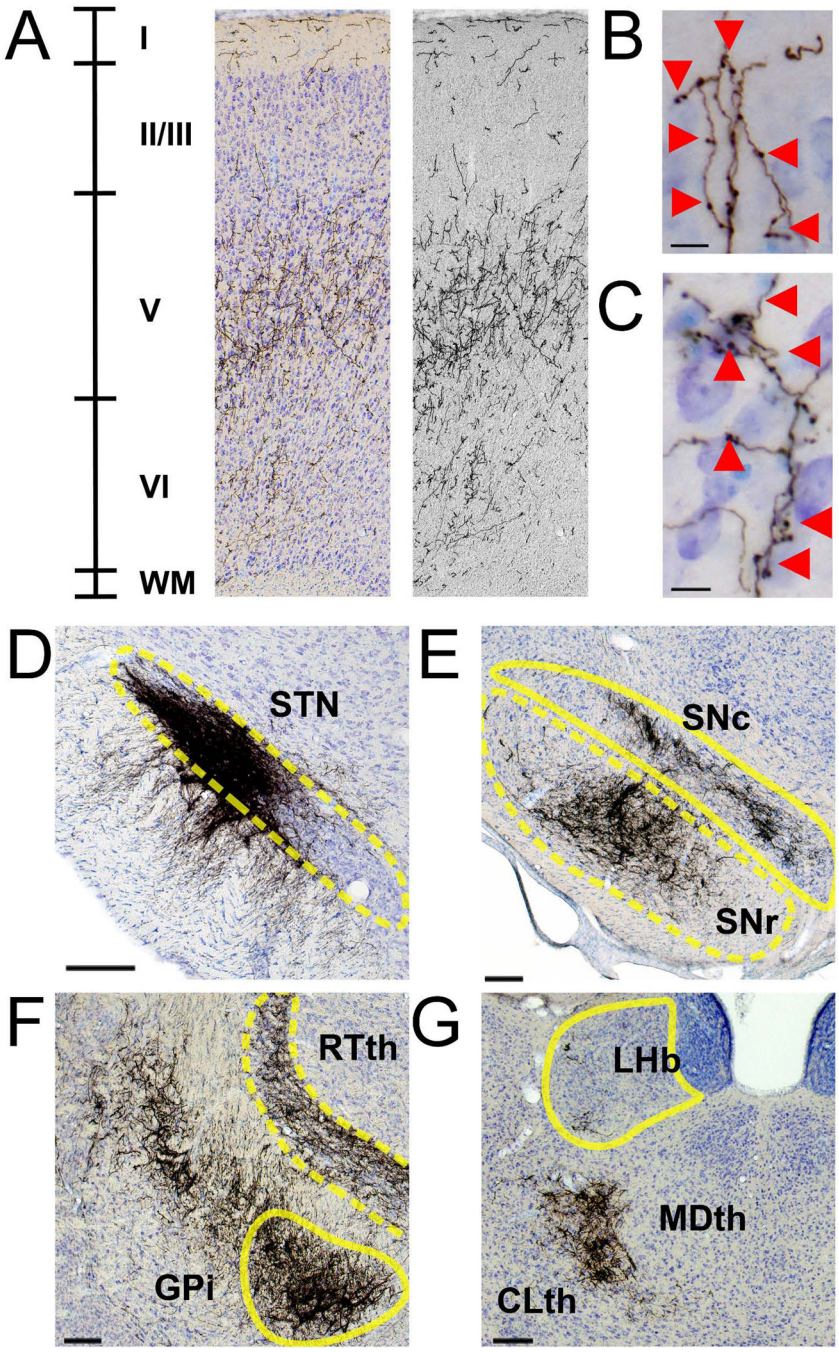

Figure 4. Additional details of GPe projections to cortex and other regions

(A) Fr2 projections from GPe, showing heavier concentration of projections to layers V/VI. (B) Closeup of pallidocortical boutons in layer I. (C) Closeup of pallidocortical boutons in layer V. Projections from tracer injection into the GPe to (D) the STN, (E) substantia nigra pars compacta (SNc) and pars reticulata (SNr), (F) GPi and reticular thalamus (rTH), (G) lateral habenula (LHb) and thalamus, including mediodorsal and centrolateral thalamus. Scale bars: B,C, 10μm; D–G 100μm

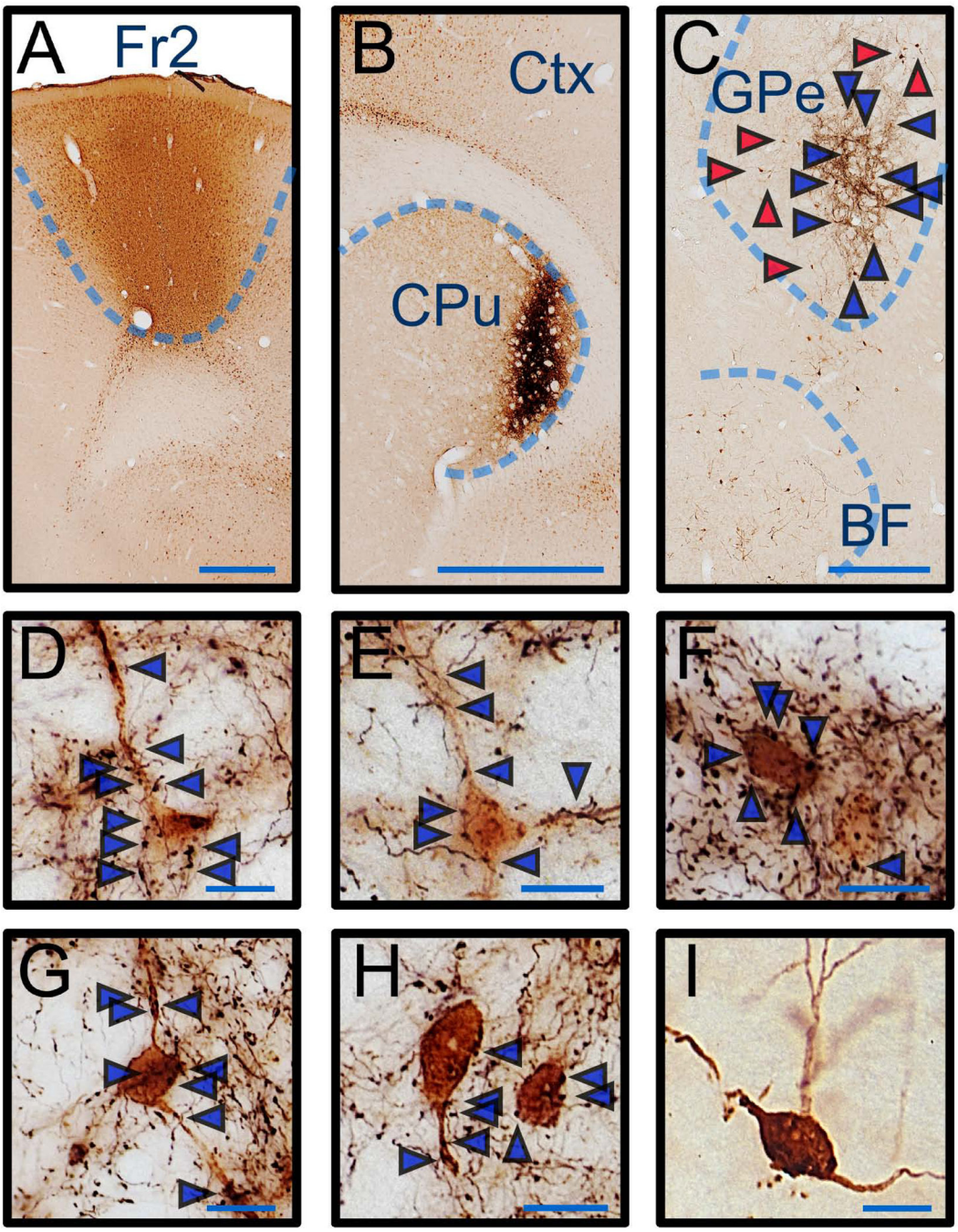

Figure 5. Retrograde tracing from Fr2 with fluorogold, stained brown, labels GPe neurons that also receive anterograde tracing from the CPu with biotinylated dextran amine (BD), stained black

(A) Injection site of fluorogold, stained brown, into Fr2. (B) Injection site of BD, stained black, into the CPu. Cortical neurons retrogradely labeled from Fr2 are also visible throughout the cortex. (C) GPe and BF neurons retrogradely labeled from Fr2 fluorogold injections. Black fibers from CPu anterograde tracing converge on the GPe, but not the BF. The restricted injection site in the CPu, and the topographic projection from the CPu to the GPe, reveals GPe neurons that project to the cortex and receive terminals from the CPu

anterograde tracer (blue arrows), as well as GPe neurons that project to the cortex but are not targeted by the tracer (red arrows). (D–H) Extended focus imaging of GPe neurons retrogradely labeled from Fr2, stained brown, and black appositions from striatum inputs, stained black. CPu appositions target the cell body and dendrites of GPe neurons (blue arrows). (I) A basal forebrain neuron retrogradely labeled from Fr2, with no CPu anterograde input. Abbreviations: globus pallidus externa (GPe), striatum (CPu), cortex (Ctx), basal forebrain (BF). Scale bars: A–C, 1mm; D–F, 20μm.

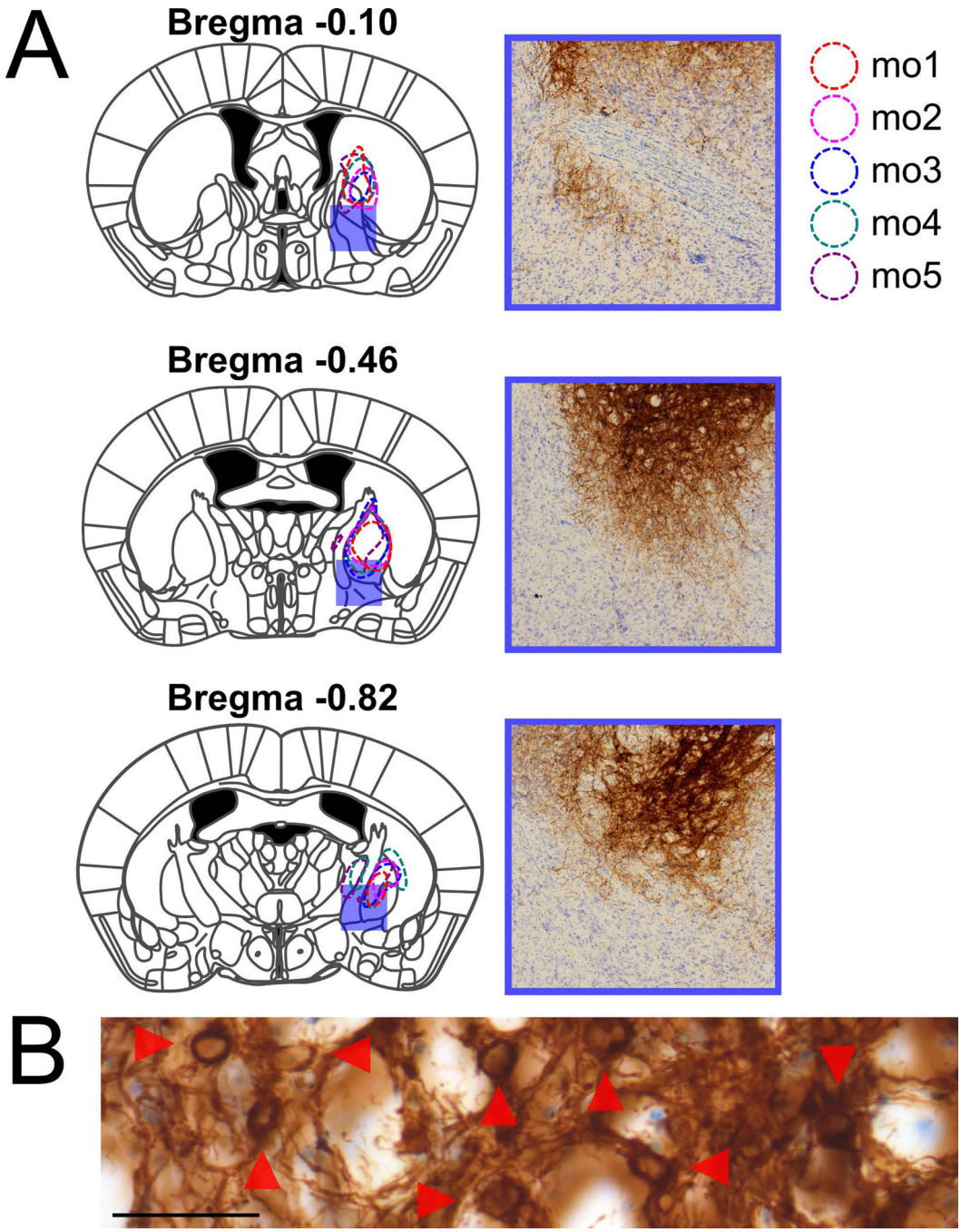

Figure 6. Injection sites of ChR2 into the mouse GPe overlayed onto a standard mouse atlas

(A) All injections were unilateral, and injection outlines are split between sides for visibility. Boxes, corresponding to case mo3 used in Figure 6, show a magnified image of the blue square zones on the injection diagram. Magnified images of the injection site in the GPe show extensive fibers, with no filled cell bodies, in the basal forebrain (BF). (B) Filled cell bodies in the GPe injection site. Scale bar: 100μm.

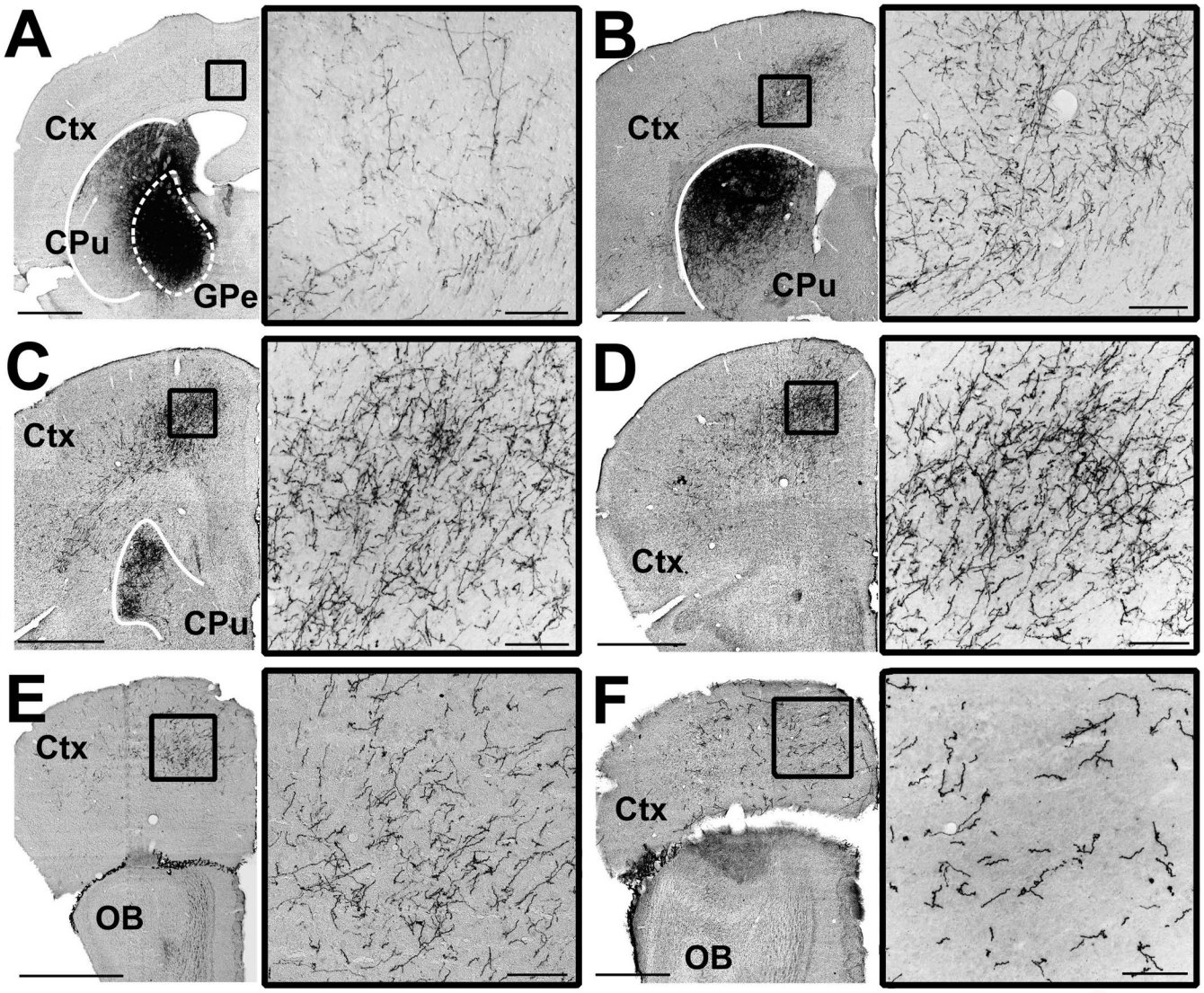

Figure 7. Cre-dependent tracer injection into the GPe of Vgat-ires-cre mice, stained brown against YFP, label GABAergic projections to Fr2 cortex at levels rostral to the injection site

(A) At the level of the injection site, heavy staining is observed in the dorsal striatum, while sparse projections and terminals can be seen passing through the corpus callosum into Fr2 (inset). (B) At the rostrocaudal level of striatum, GPe projections into both the striatum and Fr2 (inset). GPe projections to Fr2 reach their heaviest level at the rostral extent of the striatum (C,D), with dense fibers and terminals throughout layers V and VI (insets). GPe projections extend more laterally across the cortex in more rostral sections while remaining sparse along the medial wall and orbital regions (E), and reach the most rostral extent of the cortex (F). Abbreviations: globus pallidus externa (GPe), striatum (CPu), cortex (Ctx), olfactory bulb (OB). Data are presented for case Mo 3. Scale bars: A–F, 1mm; insets 100μm.

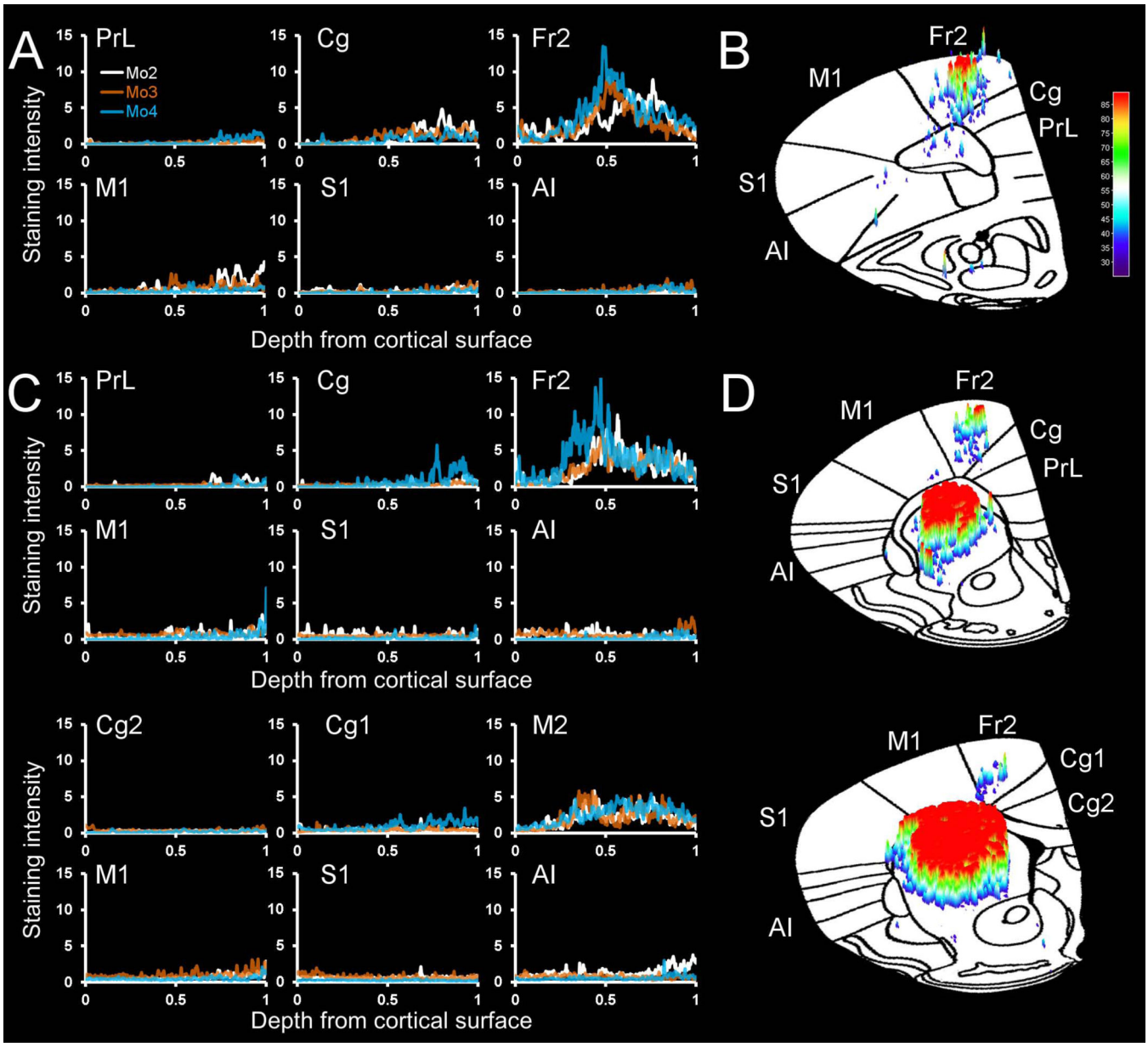

Figure 8. Quantitative mapping of GPe projections to cortical subregions in Vgat-ires-cre mice

Projection mapping in three representative mice cases, plotting normalized staining intensity against relative distance from the cortical surface to the white matter (A,C,E). Projection intensity from case Mo4 overlaid on a standardized mouse atlas (B,D,F) demonstrates the typical pattern of the GABAergic pallidocortical projection, with heavy projections to Fr2 and adjacent areas. Staining intensity of six major cortical areas are presented at the level anterior to the striatum (A–B), the anterior striatum (C–D), and striatum (E–F). Abbreviations: prelimbic cortex (PrL), cingulate cortex (Cg), frontal area 2 (Fr2), primary motor cortex (M1), primary somatosensory cortex (S1), anterior insula (AI). Colored bars in (B,D,F) reflect pixel intensity.

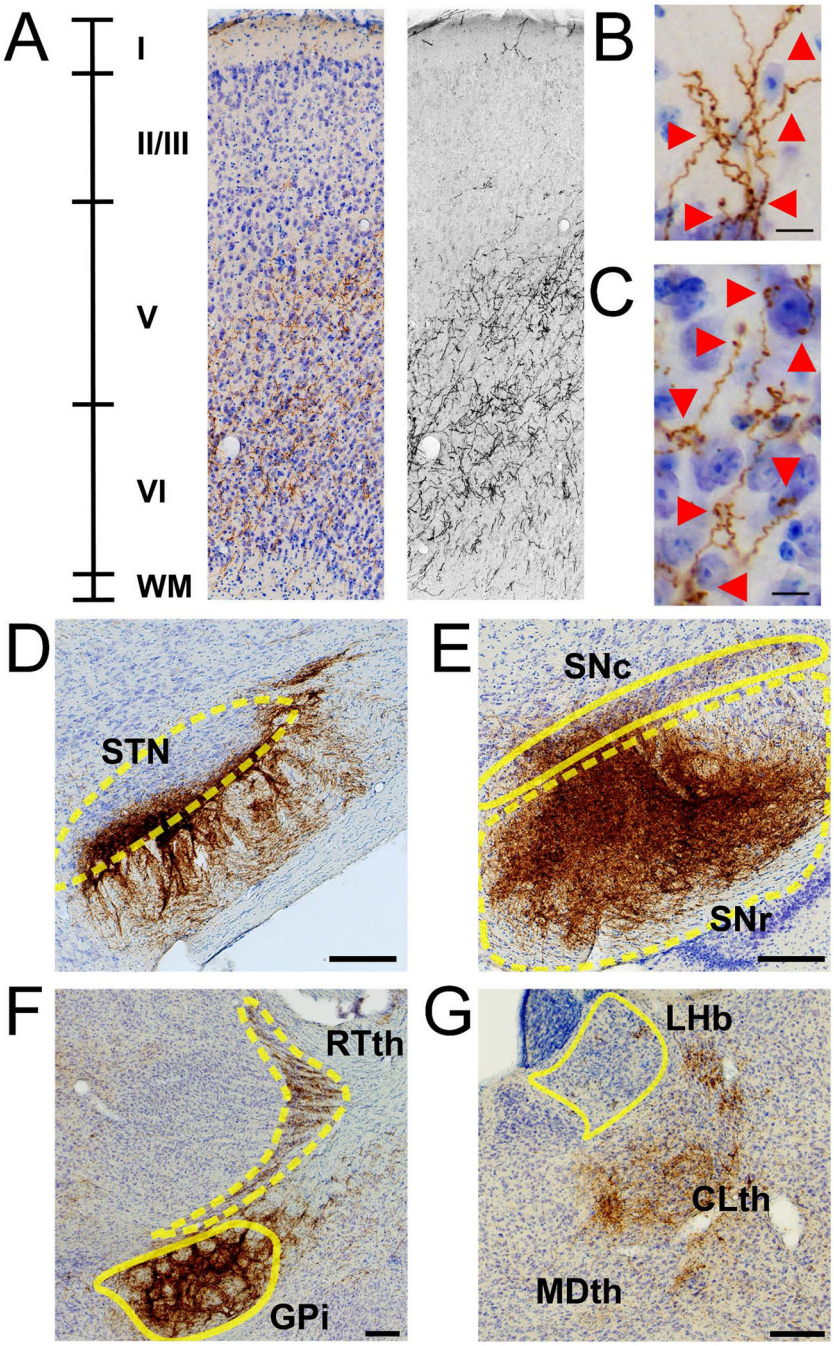

Figure 9. Additional details of GPe projections to cortex and other regions

(A) Fr2 projections from GPe, showing heavier concentration of projections to layers V/VI. (B) Closeup of pallidocortical boutons in layer I. (C) Closeup of pallidocortical boutons in layer V. Projections from tracer injection into the GPe to (D) the STN, (E) substantia nigra pars compacta (SNc) and pars reticulata (SNr), (F) GPi and reticular thalamus (rTH), (G) lateral habenula (LHb) and thalamus, including mediodorsal and centrolateral. Scale bars: B,C, 10μm; D–G 100μm.

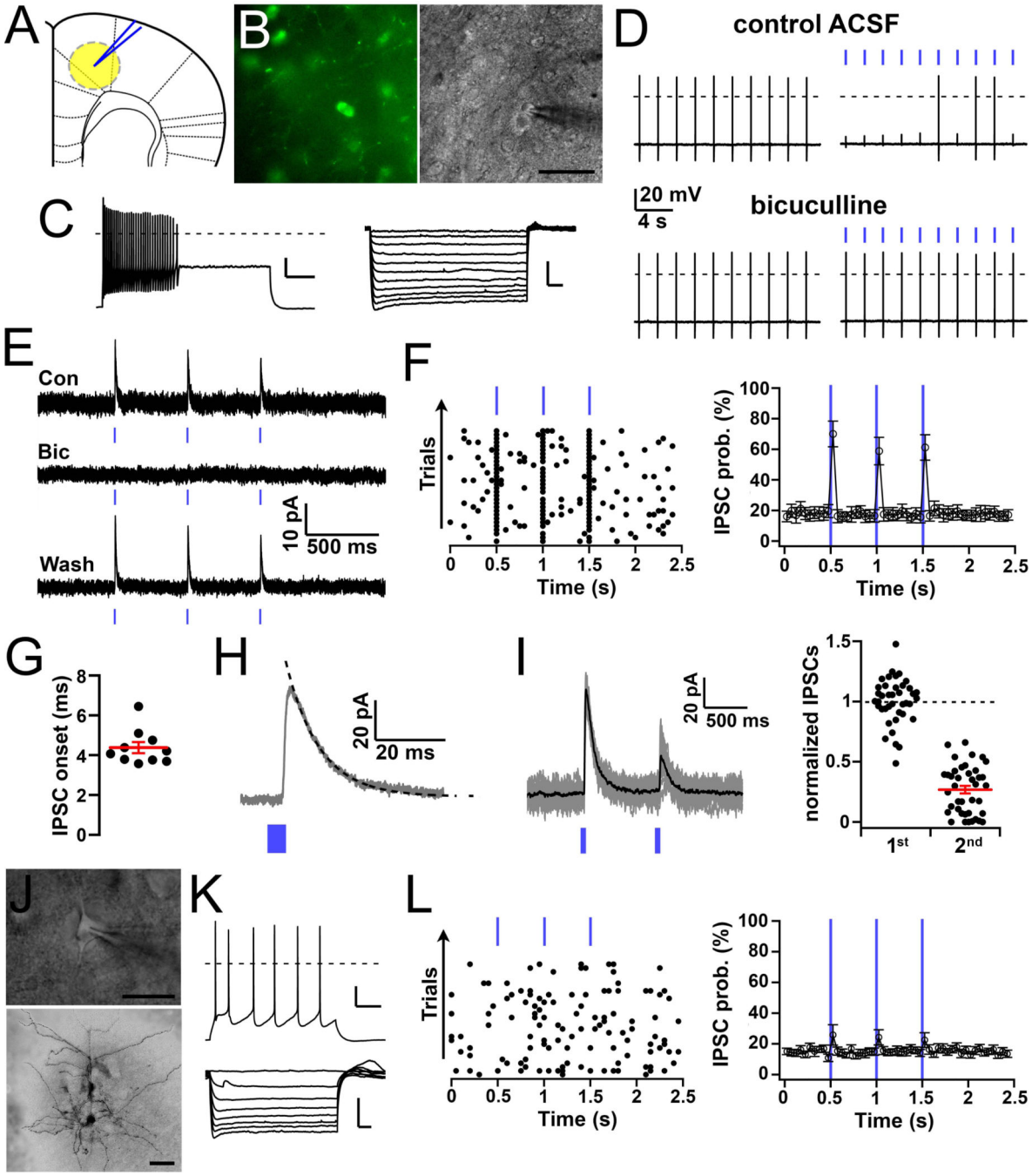

Figure 10. Photostimulation of GP^{Vgat} projections evoke GABA release onto Fr2 GABAergic interneurons

(A) Scheme of a coronal recording slice containing Fr2 cortex and the location of our recordings. (B) Photomicrographs showing GFP(+) neurons in layer V/VI from a *Vgat*-ires-cre-GFP mouse (left) and visualized under IR-DIC system during whole-cell recordings (right; scale bar: 50 μm). (C) Firing properties in response to depolarizing and hyperpolarizing current steps of a representative GFP(+) neuron that responded to photostimulation of the GP^{vgat} projections. These neurons respond to depolarizing current

steps (+300 pA, from −75 mV; top trace) with a fast and high frequency firing and with large AHP, and they respond to hyperpolarizing pulses (−20 pA, from −40 mV; bottom traces) with a small voltage-dependent rectification and a small depolarizing sag suggesting the presence of an inwardly-rectifying I_K and an I_h (scale bars: 20 mV and 200 ms; dashed line: 0 mV). (D) Photostimulation of ChR2-expressing GPe^{Vgat} axons evokes GABA release and inhibits action potential firing of GFP(+) neurons of the Fr2 cortex and this effect is blocked by bicuculline-methiodide (10 μM). Action potentials were evoked by 5ms current pulses (80 pA). (E) In voltage-clamp recordings photostimulation evokes $GABA_A$–mediated IPSCs in Fr2 GFP(+) neurons. Photoevoked IPSCs (average of 25 trials) were recorded at −40 mV in control ACSF (Con), in bicuculline (Bic), and following wash-out of bicuculline (wash). (F) A representative raster plot of IPSCs (left panel; 50 ms bin) and average IPSC probability in all recorded Fr2 GFP(+) neurons following photostimulation of $GPe^{Vgat}\rightarrow Fr2^{GFP(+)}$ pathway (right panel; 50 ms bin; n = 17 neurons; S.E.M). (G) Onset delay of $GABA_A$-mediated IPSCs in Fr2 GFP(+) neurons (n = 10; mean ± S.E.M. in red). (H) Photo-evoked IPSC decay was fitted with a single exponential (grey, average IPSCs from 30 traces; black dotted trace, single exponential fits correlation coefficient = 0.995; weighted decay time constant = 9.67 ms). (I) Paired-pulse test (80 ms inter-light pulse interval) showed significant paired-pulse depression of the photoevoked IPSCs in Fr2 GFP(+) neurons (left panel; grey traces: single 20 trials; black trace: average IPSCs). Summary graph (right panel; 40 trials from 2 neurons). IPSCs are normalized over average 1^{st} pulse IPSC amplitude (mean ± S.E.M. in red). (J) Two representative pyramidal cells that did not respond to photostimulation of the GP^{vgat}, one visualized under IR-DIC system during whole-cell recordings (top panel; scale bar: 20 μm) and one labeled with ABC-DAB-nickel staining of biocytin injected during whole-cell recordings (bottom panel; scale bar: 50 μm) (K) These neurons show the typical firing properties of cortical pyramidal cells including a fast initial adaptation followed by regular firing pattern (top trace; depolarizing current pulses +120 pA, from −65 mV; scale bar: 20 mV and 200 ms; dashed line: 0 mV), a significant voltage-dependent rectification and a small depolarizing sag suggesting the presence of an large inwardly-rectifying I_K and a small I_h (bottom traces; hyperpolarizing current pulses −40 pA, from −60 mV; scale bar: 20 mV and 200 ms; dashed line: 0 mV). (L) The majority of Fr2 pyramidal cells and did not respond to photostimulation (16 out of 19 recorded Fr2 pyramidal cells). A representative raster plot of IPSCs in a Fr2 pyramidal cell (left panel; 50 ms bin), and average IPSC probability in all recorded Fr2 pyramidal cells following photostimulation of $GPe^{Vgat}\rightarrow Fr2^{pyramidal}$ pathway (right panel; 50 ms bin; n = 19 pyramidal cells; S.E.M). In all the recordings we used 5 ms blue-light pulses indicated by blue bars at the top or the bottom of the recording traces.